Available online at www.sciencedirect.com
SCIENCE DIRECT®
PERGAMON
International Journal of Heat and Mass Transfer 46 (2003) 1873–1878
International Journal of HEAT and MASS TRANSFER
www.elsevier.com/locate/ijhmt

# Gas jet heat release inside a cylindrical cavity

K. Kessaev [a], R. Vidal [b], M. Niwa [b,*]

[a] Moscow Aviation Institute (MAI), 125871 Moscow, Russia
[b] Instituto de Aeronáutica e Espaço (IAE), 12228-904 S.J. Campos, SP, Brazil

Received 14 August 2002

**Abstract**

It is known that inside a cylindrical cavity placed at the way of an underexpanded jet, pressure oscillations accompanied by heat release can be excited. In spite of many works conducted in the past, some questions still remain about the heating mechanism, mainly due to the experimental difficulties associated with the flow structure of an underexpanded jet. The experimental results presented in this paper show that a drastic heating takes place when a cavity, filled by jet, exhibits cyclical oscillations of pressure, where the minimum cavity pressure corresponds to the level of ambient pressure outside the cavity.
© 2003 Elsevier Science Ltd. All rights reserved.

## 1. Introduction

Sprenger's study in 1954 [1] showed that an underexpanded gas jet can excite, inside a cylindrical cavity, pressure oscillations accompanied by intense heat release at the bottom, which the temperature can be several times higher than the jet stagnation temperature. In spite of much attention given to this phenomenon to clarify the reason of heating, the understanding of the whole mechanism remains incomplete up to the present day. One of the reasons for this poor advance is related to the complexity of flow structure of an underexpanded gas jet, which introduces difficulties for investigation. Meanwhile, the mechanism of heat generation continues to arouse also an applied interest, particularly for propellant ignition in rocket engines [2–5].

When in 1959, shock wave propagation was observed inside a cylindrical cavity through the shadowgraphs [6], the mechanism of heat release was explained through the energy dissipation in shock waves [7,8]. On this basis, a first attempt to evaluate the limiting temperature was made [9], however the predicted level was much higher than the measured one.

The experimental investigation conducted by Thompson [10] showed that pressure oscillations with high amplitudes are accompanied by reflected shock waves leaving the cavity, and these oscillations occur near fundamental acoustic frequency and are dictated by a periodical jet entry into the cavity with a following back flow towards the jet. In the succeeding years, the scheme wherein a cylindrical cavity is regarded as a pulsating shock tube, was used by many authors for theoretical analysis of jet–cavity interaction [11–16].

Further experimental investigations showed that depending on the nozzle stagnation pressure and on the spacing between the nozzle exit and the cavity inlet, the heat release can occur both with oscillations at about the cavity fundamental acoustic frequency and at higher frequencies [17,18].

Sarohia and Back [18], in particular, investigated experimentally the interaction of a round nozzle jet with a square-section cavity over a wide range of nozzle pressure ratio, at atmospheric ambient pressure. According to their conclusions, the intense gas heating near the cavity endwall results from a cumulative heat addition to the trapped gas by dissipative energy generated by irreversible process across the compression wave fronts. However, using a square-section cavity to visualize the inner flow shadows, they did not investigate some fundamental aspects related to the cavity inlet configuration.

* Corresponding author. Tel.: +55-12-3947-4600; fax: +55-12-3947-4621.
*E-mail address:* niwa@iae.cta.br (M. Niwa).

0017-9310/03/$ - see front matter © 2003 Elsevier Science Ltd. All rights reserved.
PII: S0017-9310(02)00438-6

**Nomenclature**

| | | | |
|---|---|---|---|
| $D$ | diameter | *Subscripts* | |
| $N$ | nozzle pressure ratio $P_0/P_1$ | c | cavity |
| $P$ | pressure | t | throttle orifice |
| $T$ | increment of temperature | 0 | nozzle inlet |
| $X$ | distance (spacing) between nozzle outlet and cavity inlet | 1 | chamber |
| | | 3 | cavity endwall |

In the present work, a round nozzle jet—cylindrical cavity system was experimentally investigated to define the conditions of most intense heating and to clarify the involved physical mechanism. Discussions on the flow structure of an underexpanded jet are also presented for the sake of clarity of the purpose of the present experiments.

## 2. Underexpanded jet structure

An underexpanded gas jet issued from a round nozzle has a complicated flow structure [19]. Since the jet is the carrier of power in a jet–cavity system, it is the governing factor in the system and thus, to define a correct experimental scheme, the flow structure of an underexpanded jet is noteworthy.

A jet assumes a supersonic velocity when it expands through the Prandtl–Mayer flow around a nozzle edge. In the downstream, the radial velocity of the gas changes its direction several times—from the longitudinal axe to the periphery and vice versa, until it becomes negligibly small owing to the energy dissipation. Such a flow peculiarity provokes deformations in the stream boundaries and forms a jet as a sequence of two or more barrel-shaped structures. With increase in the nozzle pressure ratio, shocks are generated inside barrel-shaped structures. Typical barrel-shaped structures and shocks at different nozzle pressure ratio can be observed, for example, in the free-jet shadowgraphs obtained by Sarohia and Back [18].

An arrangement of shocks is shown schematically in Fig. 1. The shock 1 (named as incident shock) is conditioned by a radial supersonic gas spreading; downstream of this shock the gas flow at the jet periphery (streamline 2) retains its supersonic velocity, and is kept under the local ambient pressure. In the shock 3 (named as reflected shock) the periphery flow once again losses partially the velocity, so that the pressure inside the flow increases above the ambient medium, but the flow keeps its supersonic velocity. In the normal shock 4 (named as Mach disk) the core of the jet is turned into subsonic flow. As a result, combination of two flows appears at the downstream of Mach disk and reflected shock: a

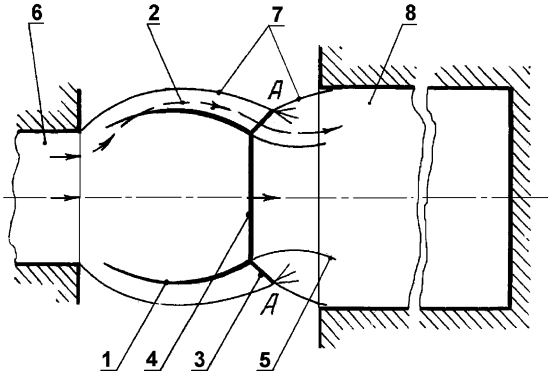


Fig. 1. The scheme of jet–cavity system. (1) incident shock; (2) periphery streamline; (3) reflected shock; (4) Mach disk; (5) mixing layer; (6) nozzle; (7) jet boundary; (8) cavity.

supersonic annular flow surrounding a subsonic flow at the jet core. Both flows have the same static pressure and are separated by the mixing layer 5. Mach disk and reflected shock close the first barrel-shaped structure, and since the jet pressure in the downstream remains higher than the ambient pressure, the jet begins a new expansion turning in rarefied waves issued out from the circle line AA. Since the periphery flow behind the reflected shock is oriented to the axe, the mixing layer forms a tapered duct, wherein the subsonic central flow is accelerated to the sound velocity. Then, following the periphery flow influence, the mixing layer forms an expanded duct, in which the central flow assumes a supersonic velocity. In the sequence, both of supersonic flows lose energy in the shocks of the second barrel-shaped structure, then in the third, as long as the jet pressure is high enough [19].

Fig. 1 depicts also a cavity 8, which can be placed at different distance $X$ relatively to the nozzle outlet. Knowing that a jet can excites pressure oscillations and heat release when a cavity is positioned some distances away from the nozzle, behind Mach disks, with the most intensive heating behind the first Mach disk [1], and considering that the underexpanded jet is formed by two concentric flows with dissimilar velocities, there are reasons to investigate the influence of both nozzle–cavity

distance and cavity diameter on the heating up. The experimental procedure and apparatus were developed for these purposes.

## 3. Test setup

Fig. 2 shows a schematic drawing of the experimental unit with computer-controlled gas-feeding line and measuring chains. The unit's elements, nozzle 2, housing 3 and tube 4 are centered on a chamber located inside the body 1. On one of the chamber face, the round nozzle 2 with diameter $D_0$ of 3.85 mm is tightly fixed, and on the opposite side, in line with the nozzle, the housing 3 is inserted into the body by thread, so that it can be moved along the axe at 1.0 mm per rotation of 360 degrees. Inside the housing a thick-walled aluminum tube 4 of 15 mm external diameter and 45 mm length is positioned. One side of the tube is facing the nozzle while the pressure transducer $P_3$, as an endwall, plugs the other. The pressure transducer $P_3$ forms a cylindrical cavity inside tube 4 and at the same time is used to record the pressure oscillations $P_3$ at the cavity endwall. The internal diameter of the tube corresponds to the cavity diameter $D_c$, which can be 3.0, 4.0, 6.0 and 7.0 mm.

Depending on the test aim, the cavity endwall can be formed by a temperature sensor $T_3$, instead of pressure transducer $P_3$, which is an aluminum plug supplied with a standard Cr–Al thermocouple. The thermocouple signal $T_3$ allows to evaluate the heat release inside the cavity at a position 1.0 mm away from the endwall.

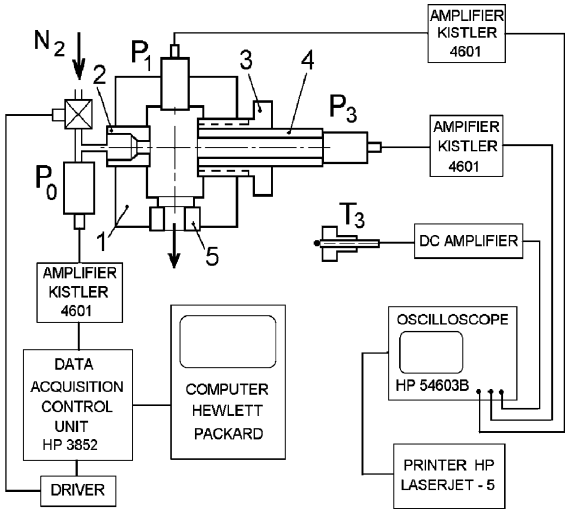


Fig. 2. Experimental setup. (1) Body; (2) nozzle; (3) housing; (4) tube; (5) throttle orifice; $P_0$, $P_1$ and $P_3$ pressure transducers; $T_3$ temperature sensor.

To exhaust the gas from the chamber there is a drain hole with a throttle orifice 5, which can have different diameters $D_t$, of 8.0, 9.0 and 10 mm. By changing the throttle orifices, it is possible to change the chamber pressure $P_1$ and to obtain a value of nozzle pressure ratio $N$ around 6.0, wherein the large-amplitude oscillations take place [16,18]. The pressure transducer $P_1$ detects the chamber pressure $P_1$.

Every single test is prepared in the following sequence: The housing 3 is supplied with the thick-walled tube 4 of a given diameter $D_c$, assembled with the pressure transducer $P_3$ (or with the temperature sensor $T_3$), and screwed into the body 1 at a distance $X$ from the outlet of nozzle 2. Finally, the throttle orifice 5 of tested diameter $D_t$ is mounted into the chamber drain hole.

Piezoresistive pressure transducers, the Kistler type 4075 A50, with the Kistler piezoresistive amplifiers type 4601 are used to detect the pressures $P_0$, $P_1$ and $P_3$. As a transduction element, they have a silicon sell with pressure-sensitive resistors diffused in and interconnected to form a fully active Wheatstone bridge. The specific properties of the silicon sell make the piezoresistive transducers equally suited for measuring constant pressures as well as transient pressures rapidly changing at a frequency up to 100 kHz and operating at a temperature range of 300–400 K.

The computer control of the tests was executed in accordance with the specific programs and through the Data Acquisition/Control Unit, Type Hewlett-Packard 3852. The signals $P_1$, $P_3$ and $T_3$ were recorded and displayed by a digital oscilloscope Type HP 54603B, and the signal $P_0$ was recorded by a data acquisition system. The measurement system recorded all information with accuracy of 1%. The duration of a single test with pressure oscillation records was limited to 100 ms to prevent overheating of the transducer $P_3$.

All the tests were performed under a fixed jet flow condition: the working gas nitrogen at a temperature of about 300 K and at a nozzle stagnation pressure $P_0$ of 12.8 bar. Depending on the throttle orifices diameters $D_t$, the chamber pressure $P_1$ can be kept in the range from 1.9 to 2.9 bar.

## 4. Test results and discussion

Fig. 3 shows, as a typical example of measurement, the simultaneous records of pressures $P_3$ and $P_1$ for a case that a jet interacts with a cavity $D_c$ of 3.0 mm and a throttle orifice $D_t$ of 9.0 mm. Records were made for various nozzle–cavity distances.

Records of Fig. 3(A) show the oscillation developments after the gas-feeding valve is turned on. The gas flow rate achieves a steady state condition after 25–30 ms in all the tested conditions.

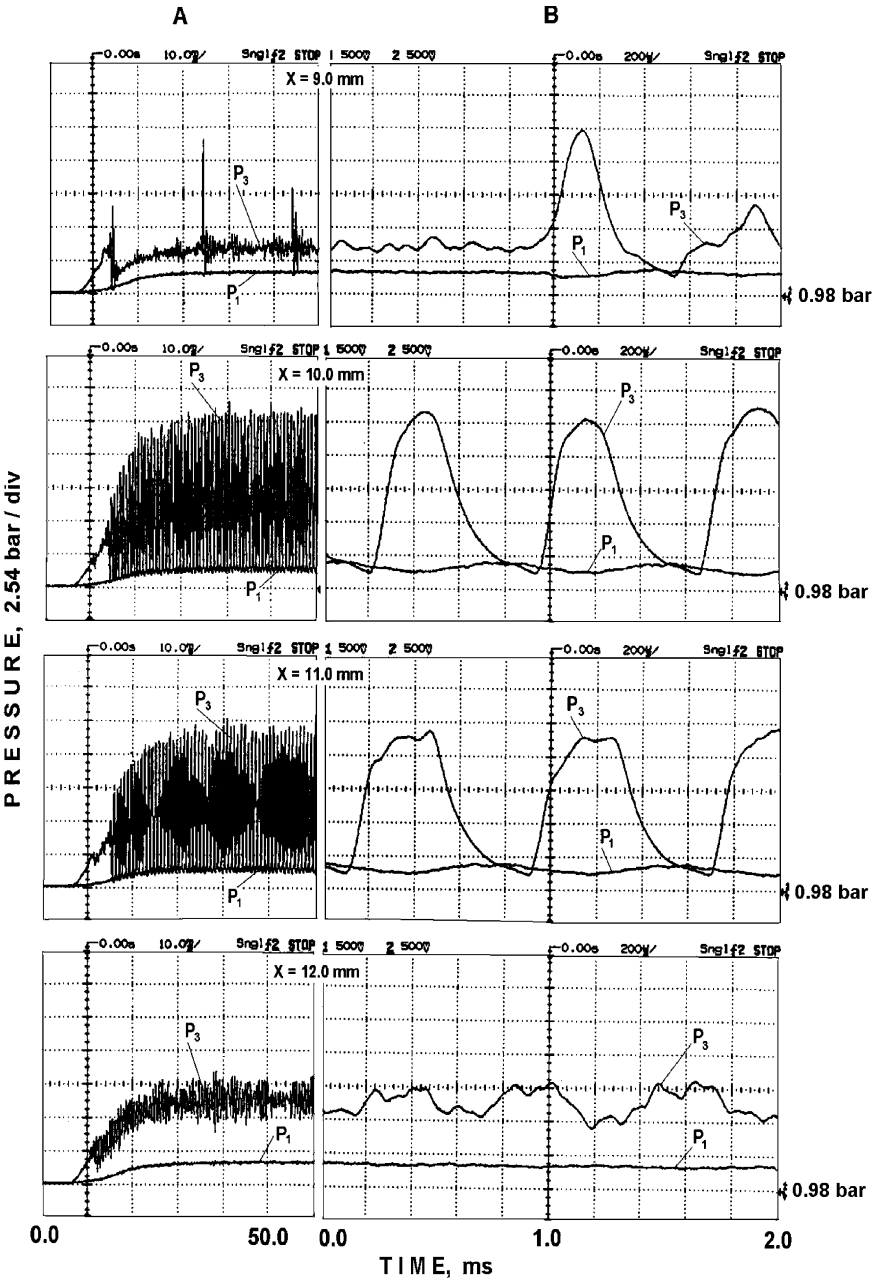


Fig. 3. Records of pressure oscillations $P_1$ and $P_3$ at different distances $X$ from the nozzle with $D_0$ 3.85 mm and $D_t$ 9.0 mm.

The records of Fig. 3(B) refer to the steady-state conditions for the corresponding signals $P_3$ and $P_1$, but at a larger scale of time. It makes possible to observe a single wave configuration and to evaluate the frequencies and the feature of oscillations.

It is evident from Fig. 3 that:

- At some distance between the nozzle outlet and the cavity inlet ($X = 9.0$ mm) the pressure oscillations $P_3$ emerge, and with a further increase in the distance, the amplitude of $P_3$ increases, reaches a maximum and then die away ($X = 12.0$ mm).
- Large-amplitude oscillations of $P_3$ ($X = 10.0$ and 11.0 mm) are not harmonic: after a fast pressure rising a slower abatement is seen.
- Large-amplitude oscillations of $P_3$ are accompanied by low-amplitude oscillations of $P_1$, which in every cycle assumes a minimum, while $P_3$ assumes a maximum.

- The largest values of compression ratio $P_{3\max}/P_{3\min}$ take place when $P_{3\min} = P_{1\min}$.
- Frequencies of large-amplitude oscillations are in the range of 1350–1400 Hz, which is lower than the fundamental acoustic frequency of the investigated cavity.

Precisely the same features are also seen from the records of $P_3$ and $P_1$ obtained with cavities $D_c$ of 3.0, 4.0, 6.0 and 7.0 mm, combined with throttle orifices $D_t$ of 8.0, 9.0 and 10.0 mm.

From the above-mentioned results, a scheme of a single large-amplitude cycle can be drawn: The jet enters into the cavity, compresses the gas situated there, at ambient pressure $P_{1\min}$, up to the pressure $P_{3\max}$, and then the compressed gas expands to the initial pressure $P_{1\min}$, so that the entering external jet gas is forced out completely from the cavity. The main characteristic of the large-amplitude oscillations, as shown in Fig. 3, is the equality $P_{3\min} = P_{1\min}$.

Considering the irregular shape of pressure oscillation records, a heat release inside the cavity should be expected. Fig. 4 shows an example of records of temperature increment $T_3$ for 2.0 s after the gas-feeding valve is turned on. This example shows a cases when a jet interacts with a cavity $D_c$ of 3.0 mm at several distances of $X$ for a throttle orifice $D_t$ of 9.0 mm. Identical records were obtained with all combinations of cavities and throttle orifices. Throughout the tests the temperature of the thick and conductive aluminum wall of the cavities practically did not change its initial value during the first 2.0 s of heating. Thus, the value of temperature increment $T_3$ after 2.0 s of heating allows estimate the intensity of heat release inside the cavity, to evaluate the specific factors of influence.

Fig. 5 presents the curves for temperature increment $T_3$ after 2.0 s of heat release in the cavities $D_c$ of 3.0, 4.0, 6.0 and 7.0 mm, for a throttle orifice $D_t$ of 9.0 mm, at several distances $X$. The segments marked by solid lines correspond to the cavity oscillations with $P_{3\min} = P_{1\min}$. This figure allows infer that:

- The intricate plotted curves reflect the above-described complex flow structure of an underexpanded jet.
- The heat release is most intense when $P_{3\min} = P_{1\min}$.
- The heat release increases with $D_c$, evidencing the role of the periphery flow of the jet.
- Each $D_c$ requires a specific adjustment of distance $X$ for attaining the conditions for most intensive heat release.

The same experiment conducted with different throttle orifices leads to a similar result. Fig. 6 presents an example for a throttle orifice of 10.0 mm, i.e. for pressure surrounding the jet lower than that for 9.0 mm throttle orifice.

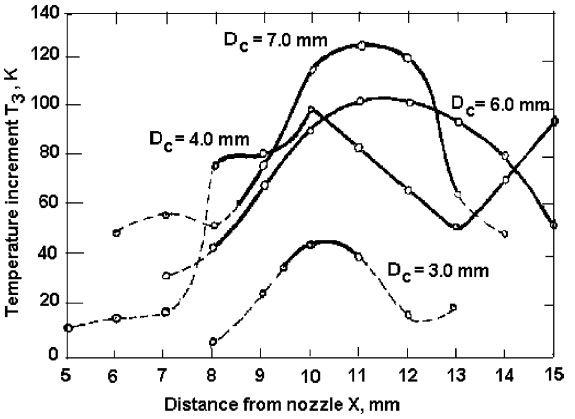


Fig. 5. Temperature increment $T_3$ for different $D_c$ and distance $X$ by $D_t$ of 9.0 mm.

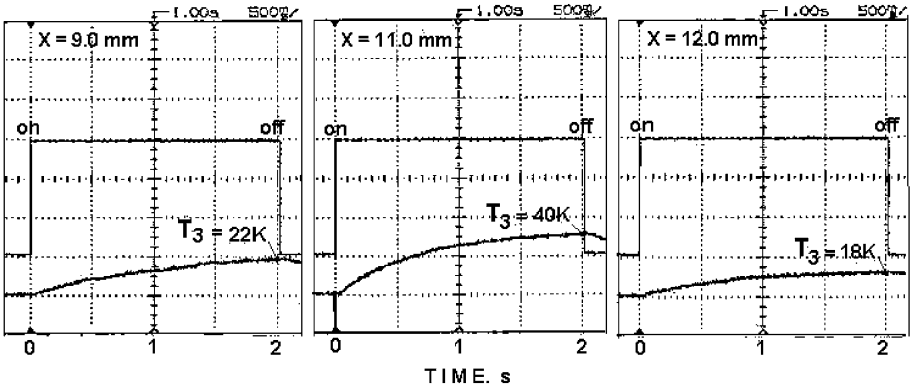


Fig. 4. Records of temperature increment $T_3$ at different distances $X$ from the nozzle with $D_0$ 3.85 mm and $D_t$ 9.0 mm.

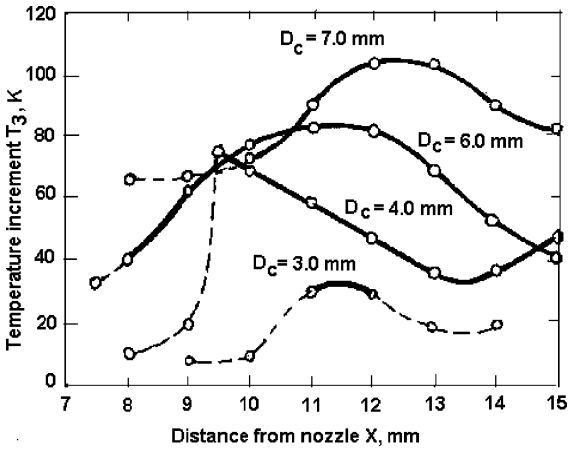


Fig. 6. Temperature increment $T_3$ for different $D_c$ and distance $X$ by $D_t$ of 10.0 mm.

## 5. Conclusions

The heat release in a gas dynamical system of an underexpanded jet and a cylindrical cavity under a fixed jet power (fixed nozzle diameter and stagnation pressure) condition was experimentally investigated with different combinations of nozzle pressure ratio, cavity diameter and nozzle–cavity distance. The main conclusions can be summarized as follows:

- The most intensive heating occurs inside the cavity when the underexpanded jet periodically intrudes deeply into the cavity and compresses the local gas, after which the compressed gas forces out the entering gas and expands to the ambient pressure.
- The jet periphery supersonic flow has determining effect on the heat release.
- Obtained experimental facts open a way for further investigations to reveal the phenomenon potentials, applied to other cavity configurations.

## Acknowledgements

The first and the third authors would like to acknowledge Moscow Aviation Institute (MAI) for the collaboration and Conselho Nacional de Desenvolvimento Científico e Tecnológico (CNPq—Brazil) for the financial support during the conduction of the present work.

## References

[1] H.S. Sprenger, Über thermische Effekte in Resonanzrohren, Mitteilungen aus dem Institut für Aerodynamik ETH, no. 21, Zürich, 1954, pp. 18–35.
[2] B. Phillips, A.J. Pavli, E.W. Conrad, A resonance igniter for hydrogen–oxygen combustors, J. Spacecraft Rockets 7 (5) (1970) 620–622.
[3] V.P. Marchese, E.L. Rakowsky, L.J. Bement, A fluid sounding rocket motor ignition system, J. Spacecraft Rockets 10 (1973) 731–734.
[4] G. Liang, G. Zhang, X. Cheng, B. Ma, Z. Zhang, Preliminary investigation on gas dynamic resonance ignition for liquid propellant rocket engine, J. Propul. Technol. 20 (4) (1999) 13–16.
[5] M. Niwa, A. Santana Jr., K. Kessaev, Modular ignition system based on resonance igniter, J. Propul. Power 17 (5) (2001) 1131–1133.
[6] I.M. Hall, C.J. Berry, On the heating effect in a resonance tube, J. Aerospace Sci. 26 (40) (1959) 253.
[7] J. Wilson, E.L. Resler Jr., A mechanism of resonance tubes, J. Aerospace Sci. 26 (7) (1959) 461–462.
[8] A.H. Shapiro, Shock waves and dissipation in a resonance tube, J. Aerospace Sci. 26 (10) (1959) 684–685.
[9] A.H. Shapiro, On the maximum attainable temperature in resonance tubes, J. Aerospace Sci. 27 (1) (1960) 66–67.
[10] P.A. Thompson, Jet driven resonance tube, AIAA J. 2 (7) (1964) 1230–1233.
[11] K.A. Morch, A theory for the mode of operation of the Hartmann air jet generator, J. Fluid Mech. 20 (1) (1964) 141–159.
[12] E. Brocher, C. Maresca, M.H. Bournay, Fluid dynamic of the resonance tube, J. Fluid Mech. 43 (2) (1970) 369–384.
[13] C.E.G. Przirembel, L.S. Fletcher, Aerothermodynamics of a simple resonance tube, AIAA J. 15 (1) (1977) 101–104.
[14] J.A. Vagramenko, V.N. Lyakhov, V.M. Ustinov, Pulsations by impinging of the stationary nongomogenous flow on a barrier, Izvestija AN USSR, Fluid Mech. (5) (1979) 64–71 (in Russian).
[15] L.I. Vereschagina, E.A. Ugrjumov, Gasdynamic and thermal characteristic calculations of a resonance tube with a supersonic jet entering, Vestnik Leningrad University (1) (1981) 59–64 (in Russian).
[16] K.V. Kessaev, Theoretical model of resonance tube, Izvestija Vusov, Aviationnaja Tekhnika (2) (1990) 49–52 (in Russian).
[17] V.M. Kuptsov, S.I. Ostroukhova, K.N. Fillipov, Pressure oscillations and gas heating by a supersonic jet entering into cylinder cavity, Izvestija AN USSR, Fluid Mech. (5) (1977) 104–111 (in Russian).
[18] V. Sarohia, L.H. Back, Experimental investigation of flow and heating in resonance tube, J. Fluid Mech. 94 (4) (1979) 649–672.
[19] V.S. Avduevsky, E.A. Ashratov, A.V. Ivanov, U.G. Pirumov, Gas Dynamics of Supersonic Nonisobaric Jets, Mashinostroenie, Moscow, 1989, pp. 1–320.